



A LETTERS JOURNAL EXPLORING
THE FRONTIERS OF PHYSICS

OFFPRINT

**Geometry-dependent conductance oscillations
in graphene quantum dots**

LIANG HUANG, RUI YANG and YING-CHENG LAI

EPL, **94** (2011) 58003

Please visit the new website
www.epljournal.org

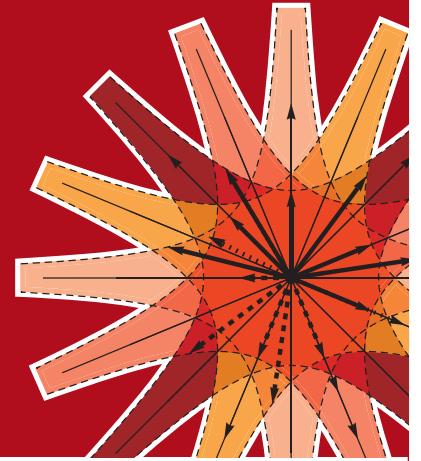


epl

A LETTERS JOURNAL
EXPLORING THE FRONTIERS
OF PHYSICS

The Editorial Board invites you
to submit your letters to EPL

www.epljournal.org



Six good reasons to publish with EPL

We want to work with you to help gain recognition for your high-quality work through worldwide visibility and high citations. As an EPL author, you will benefit from:

- 1 Quality** – The 40+ Co-Editors, who are experts in their fields, oversee the entire peer-review process, from selection of the referees to making all final acceptance decisions
- 2 Impact Factor** – The 2009 Impact Factor increased by 31% to 2.893; your work will be in the right place to be cited by your peers
- 3 Speed of processing** – We aim to provide you with a quick and efficient service; the median time from acceptance to online publication is 30 days
- 4 High visibility** – All articles are free to read for 30 days from online publication date
- 5 International reach** – Over 2,000 institutions have access to EPL, enabling your work to be read by your peers in 100 countries
- 6 Open Access** – Experimental and theoretical high-energy particle physics articles are currently open access at no charge to the author. All other articles are offered open access for a one-off author payment (€1,000)

Details on preparing, submitting and tracking the progress of your manuscript from submission to acceptance are available on the EPL submission website www.epletters.net

If you would like further information about our author service or EPL in general, please visit www.epljournal.org or e-mail us at info@epljournal.org



IOP Publishing

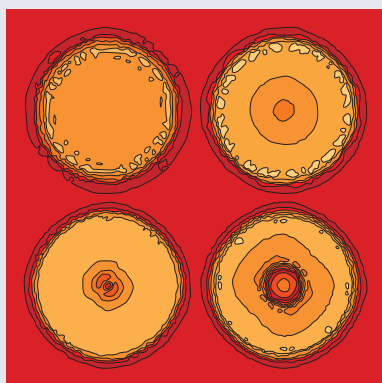
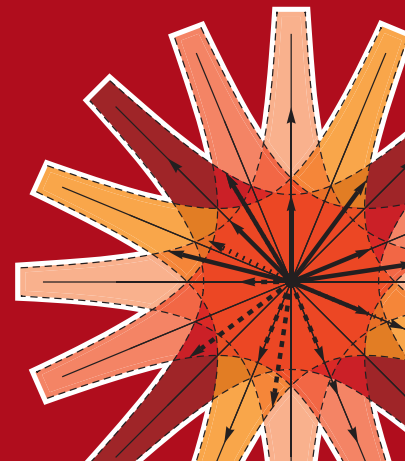
Image: Ornamental multiplication of space-time figures of temperature transformation rules
(adapted from T. S. Biró and P. Ván 2010 *EPL* **89** 30001; artistic impression by Frédérique Swist).



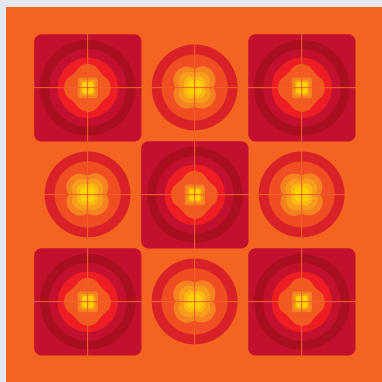
A LETTERS JOURNAL
EXPLORING THE FRONTIERS
OF PHYSICS

EPL Compilation Index

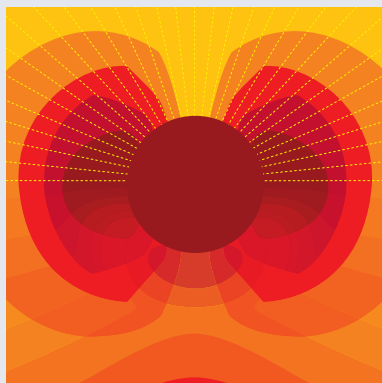
www.epljournal.org



Biaxial strain on lens-shaped quantum rings of different inner radii, adapted from **Zhang et al** 2008 *EPL* **83** 67004.



Artistic impression of electrostatic particle-particle interactions in dielectrophoresis, adapted from **N Aubry and P Singh** 2006 *EPL* **74** 623.



Artistic impression of velocity and normal stress profiles around a sphere that moves through a polymer solution, adapted from **R Tuinier, J K G Dhont and T-H Fan** 2006 *EPL* **75** 929.

Visit the EPL website to read the latest articles published in cutting-edge fields of research from across the whole of physics.

Each compilation is led by its own Co-Editor, who is a leading scientist in that field, and who is responsible for overseeing the review process, selecting referees and making publication decisions for every manuscript.

- Graphene
- Liquid Crystals
- High Transition Temperature Superconductors
- Quantum Information Processing & Communication
- Biological & Soft Matter Physics
- Atomic, Molecular & Optical Physics
- Bose-Einstein Condensates & Ultracold Gases
- Metamaterials, Nanostructures & Magnetic Materials
- Mathematical Methods
- Physics of Gases, Plasmas & Electric Fields
- High Energy Nuclear Physics

If you are working on research in any of these areas, the Co-Editors would be delighted to receive your submission. Articles should be submitted via the automated manuscript system at www.epletters.net

If you would like further information about our author service or EPL in general, please visit www.epljournal.org or e-mail us at info@epljournal.org



IOP Publishing

Image: Ornamental multiplication of space-time figures of temperature transformation rules (adapted from T. S. Bíró and P. Ván 2010 *EPL* **89** 30001; artistic impression by Frédérique Swist).

Geometry-dependent conductance oscillations in graphene quantum dots

LIANG HUANG^{1,2}, RUI YANG¹ and YING-CHENG LAI^{1,3}

¹ *School of Electrical, Computer, and Energy Engineering, Arizona State University - Tempe, AZ 85287, USA*

² *Institute of Computational Physics and Complex Systems, and Key Laboratory for Magnetism and Magnetic Materials of MOE, Lanzhou University - Lanzhou, Gansu 730000, China*

³ *Department of Physics, Arizona State University - Tempe, AZ 85287, USA*

received 9 February 2011; accepted in final form 26 April 2011

published online 27 May 2011

PACS 81.05.ue – Graphene

PACS 72.80.Vp – Electronic transport in graphene

PACS 73.63.Kv – Electronic transport in nanoscale materials and structures: Quantum dots

Abstract – Utilizing rectangular graphene quantum dots with zigzag horizontal boundaries as a paradigm, we find that the conductance of the dots can exhibit significant oscillations with the *position* of the leads. The oscillation patterns are a result of quantum interference determined by the band structure of the underlying graphene nanoribbon. In particular, the power spectrum of the conductance variation concentrates on a *selective* set of bands of the ribbon. The computational results are substantiated by a heuristic theory that provides selection rules for the concentration on the specific dispersion bands.

Copyright © EPLA, 2011

Graphene, a single layer of carbon atoms arranged in a honeycomb lattice, has attracted much recent interest [1]. Potential applications of graphene range from electronics [2] to nano-biosensors [3]. For example, due to the distinctly high mobility of charge carriers in graphene [4], nanoscale electronic devices made of graphene, such as *p-n* junctions and transistors, can be superior to their Si-based counterparts [5]. For most applications, there is a need to connect the graphene device to external voltage or current source via metal leads. Ideally, there should be zero resistance between the metal lead and the graphene. However, experiments have shown that the contact resistance can approach or even exceed the quantum resistance [6]. This indicates that some form of injection barrier must exist at the metal-graphene interface, as demonstrated in fig. 1(a), restricting the transmitting modes to a few [6,7].

In this letter, we use a zigzag graphene quantum-dot model where the size of the leads is assumed to be small to mimic the injection characteristics of a few transmitting modes and study, systematically, how the conductance of the quantum dot depends on the position of the leads (fig. 1(b)). It has been noticed that the geometry of the device can affect the electronic transport properties [7–10]. Intuitively, if the lead is located in a region where the local density of states (LDS) is low, electrons can hardly hop

out of the localized pattern to get into the lead, resulting in a small conductance [11]. Opposite situations can occur when the lead is in a different region, leading to a large conductance. Our systematic computations with varying lead positions reveal significant conductance oscillations. A heuristic analysis indicates that the oscillations are caused by standing-wave-like patterns in the quantum dot. In particular, the wave vector of the wave function follows the underlying dispersion relation. For tall and narrow quantum dots, as sketched in fig. 1(b), the relation can be approximated by the band structure of the corresponding armchair graphene ribbon when viewed vertically (*y*-direction) in the absence of leads. There are two sets of bands depending on the phase difference of the two atoms (denoted by A and B) in a unit cell. At the bottom of these bands, for one set, the wave function for A atoms has the same phase as that for B atoms. For the other set, the wave function for the two set atoms has the opposite phase, which do not contribute to the transmission as they annihilate from destructive interference. In the nanotransport literature, conductance oscillations/fluctuations are usually referred to those with respect to varying electron energy or changing magnetic field [12], the origin of which can generally be attributed to scarred or pointer states in the underlying dot structure [11]. The

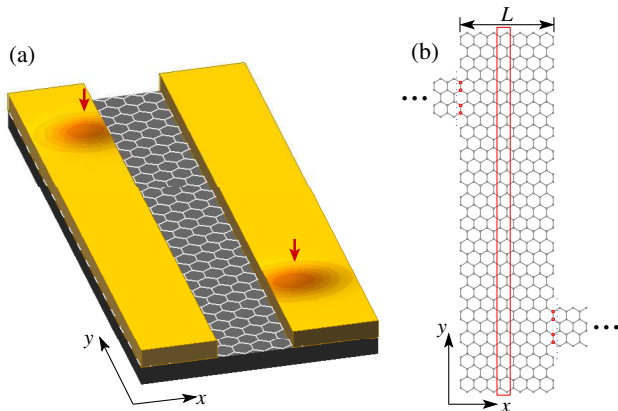


Fig. 1: (Color online) (a) A schematic graphene device with metal contacts. Surface roughness may impose injection barriers at the metal-graphene interface (as indicated by the red arrow). (b) The same device with semi-infinite narrow leads modeling the injection characteristics of a few transmitting modes. Because of the discrete lattice structure, the position of the lead can only be changed vertically in a multiple of the lattice distance, which is $\sqrt{3}a$, where $a = 0.246$ nm is the lattice constant, and $i_{L/R} = 1$ if the left/right lead resides at the bottom of the dot. The rectangles indicate a slice of N atoms, and L is the width of the device. The short dotted lines separate the dot and the leads. The circles are the boundary atoms with direct interaction with the leads. The device parameters are $i_L = 13$, $i_R = 3$, $L = 7a$, and $N = 16 \times 4$.

oscillations/fluctuations reported here are induced purely by geometrical variation in the whole device (quantum dot plus leads), caused by a different mechanism.

In our calculations we assume the leads are semi-infinite, narrow zigzag graphene ribbons supporting 8 transmission modes, which has 4×4 atoms in a slice (twice wider than the leads in fig. 1(b)). The positions of the leads can vary only in an integer multiplication of the basic lattice unit in the vertical direction. To capture the essential physics, we fix the left lead, and systematically change the position of the right lead, denoted by i_R . We employ the standard tight-binding framework and the non-equilibrium Green's function formalism to calculate the transmission T and then use the Landauer formula for the conductance G [13]. The tight-binding Hamiltonian is given by $\hat{H} = \sum (-t)|i\rangle\langle j|$, where the summation is over all pairs of nearest neighboring atoms, and $t \approx 2.8$ eV is the hopping energy [1]. In the position representation, $\langle i|j\rangle = \delta_{ij}$, thus the Hamiltonian matrix elements are given by $H_{ij} = \langle i|\hat{H}|j\rangle$, which is $(-t)$ if i and j are nearest neighbors and 0 otherwise. The interslice interaction is characterized by the coupling between the nearest neighboring pairs linking the two slices. Thus the contacts, depending on their vertical location, will link to different atoms in the dot, which will modify the Hamiltonian matrix, especially the subblock describing the interslice interactions of the boundary slices of the dot with the lead. The semi-infinite leads can equivalently be treated as a self-energy matrix

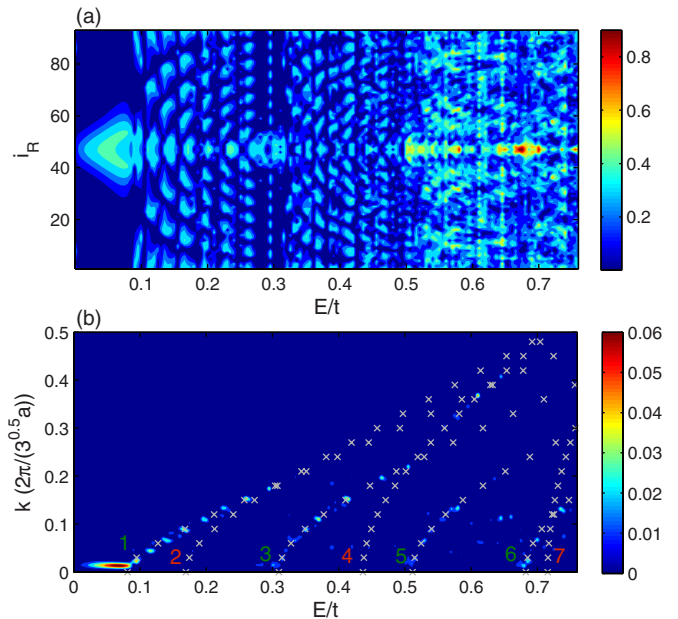


Fig. 2: (Color online) (a) Contour plot of the conductance variation \tilde{G} (in units of $2e^2/h$) as a function of the right-lead position i_R and the Fermi energy. (b) Power spectrum (arbitrary units) of the conductance variation \tilde{G} in the $(k, E/t)$ -plane. The geometric parameters of the device are $L = 10a$, $N = 96 \times 4$, and $i_L = 47$ (the middle of the device). The crosses represent the bands for the corresponding vertical ribbon where the value of the wave vector is doubled.

of the atoms in the dot with direct interactions with the leads (small circles in fig. 1(b)), which is included in the Hamiltonian and Green's function for calculating the transmission [13].

To characterize the dependence of the conductance on the lead position, for each Fermi energy E , we calculate the quantity $\tilde{G}(i_R, E) = G(i_R, E) - \langle G(i_R, E) \rangle_{i_R}$. Figure 2(a) shows, for a zigzag dot, a contour plot of the conductance variation \tilde{G} in the two-dimensional parameter space of the right lead position i_R and the Fermi energy E . The high conductance region forms a well-pronounced pattern, which is robust in that similar patterns persist for varied dot size and/or left-lead position. For fixed left-lead position and Fermi energy, the conductance depends sensitively on the position i_R of the right lead. For many Fermi-energy values, the conductance variations are in fact periodic. To characterize this periodic pattern, we perform its spatial Fourier transform with respect to i_R . The results are shown in fig. 2(b). The contour plot of the power spectrum reveals a striking pattern of well-pronounced line segments. As the Fermi energy is varied, a dominant frequency can occur but only for a small set of energy values, signifying periodic conductance oscillations with the lead position for these energy values. For other energies, such a dominant frequency is absent, indicating random conductance fluctuations with the lead position.

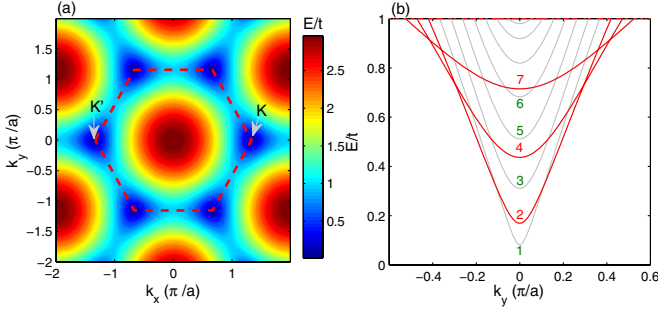


Fig. 3: (Color online) (a) Contour plot of the dispersion relation of an infinite graphene flake with the x -direction being zigzag. The dashed line indicates the first Brillouin zone. The \mathbf{K} and \mathbf{K}' points are $(4\pi/(3a), 0) = (K, 0)$ and $(-K, 0)$, respectively. (b) Calculated band structure for the armchair nanoribbon with $L = 10a$ (k_y -direction in (a)). The gray (lighter) curves are for $k_x > K$. The red (darker) ones are for $k_x < K$. The labels of the bands are the same as that in fig. 2(b).

The overlaid crosses in fig. 2(b) represent the band structure of the corresponding vertical ribbon for which the leads are removed¹. The coincidence of the line segments and the crosses indicates scarring of the power spectrum of \tilde{G} on the energy bands. We observe that, although the bright spots in the power spectrum follow the band structure, not all the bands are occupied. As we shall demonstrate below, this *selective scarring* phenomenon can be explained by the phase properties of the wave functions.

We now provide an explanation for geometry-dependent conductance fluctuations in graphene quantum dots. First, consider an infinite graphene flake. Figure 3(a) shows a contour plot of the energy dispersion relation for the infinite graphene flake, where \mathbf{K} and \mathbf{K}' are the two Dirac points. For the quantum dot we studied, removing the leads results in an armchair ribbon in the y -direction. Figure 3(b) shows its dispersion relation. Note that there are two sets of bands for the armchair ribbon. The first set is for $k_x > K$, which are the gray (lighter) curves in fig. 3(b). The other set is for $k_x < K$, which are the red (darker) ones. Regarding the isolated quantum dot as an armchair nanoribbon in the y -direction, the wave function for wave vectors close to the Dirac point \mathbf{K} has the form [14] $\psi(x, y) = e^{ik_y y} [\phi_A(x), \phi_B(x)]^T$. The Hamiltonian is given by

$$H_{\mathbf{K}} = v_F(\mathbf{p} \cdot \boldsymbol{\sigma}) = v_F \begin{pmatrix} 0 & p_x - ip_y \\ p_x + ip_y & 0 \end{pmatrix},$$

where $\boldsymbol{\sigma}$ denotes the Pauli matrices. The eigen-equation $H\psi = E\psi$ yields

$$\phi_A(x) = \frac{-i\hbar v_F}{E} (\partial_x + k_y) \phi_B(x) \quad (1)$$

¹The value of the wave vector for the band structure is doubled because the probability density function determining the transmission is the square of the module of the wave function. As a result, the frequency of the transmission oscillations as the right lead moves is twice as that of the wave function in the y -direction.

and

$$\phi_B(x) = \frac{-i\hbar v_F}{E} (\partial_x - k_y) \phi_A(x). \quad (2)$$

Combining eqs. (1) and (2), we have $\phi_B(x) = (\hbar^2 v_F^2 / E^2) (k_y^2 - \partial_x^2) \phi_B(x)$. Applying the boundary condition of the armchair ribbon, the solution is $\phi_B(x) = A e^{ik_n x}$, where $k_n = n\pi/L - 4\pi/(3a)$ and L is the width of the ribbon [14]. Substituting this solution back to eq. (1), we have

$$\phi_A(x) = \frac{-i\hbar v_F}{E} (ik_n + k_y) \phi_B(x). \quad (3)$$

Now reexamine fig. 2(b). The bands can be characterized by their cross points with the energy axis, which are located at the bottom of the bands (fig. 3(b)). In this region, $k_y \approx 0$ and $E \approx v_F \hbar |k_n| > 0$, so eq. (3) becomes

$$\phi_A(x) \approx \frac{\hbar v_F k_n}{E} \phi_B(x) = \text{sign}(k_n) \phi_B(x). \quad (4)$$

The same holds for the other Dirac point. We see that, depending on the value of k_n or the location of k_x (on the right or left side of the Dirac point \mathbf{K}), the wave function of A atoms may have the same phase or the opposite phase as that of B atoms, corresponding to bonding or antibonding states [15] when the energy surpasses the corresponding band. This has been verified by numerical calculation of the wave functions of armchair ribbons.

It can now be argued that only the bands for which the wave functions for A and B atoms possess the same phase contribute to the conductance of the quantum dot, while the bands with opposite phases have no contributions. Our idea is to use the mode matching technique in the calculation of the transmission [16]. In particular, the transmission of the quantum dot is nonzero if the modes in the left lead match those in the dot, which also match the modes in the right lead. The leads are narrow zigzag ribbons. The wave functions of A and B atoms are symmetric under reflection with respect to the vertical direction. In other words, they possess the same phase under a reflection. Since the width of the leads is much smaller than the vertical scale of the quantum dot, the wave functions of the dot in the lead region can be regarded as constants. Mode matching is the sum of the cross integral between the wave functions of A and B atoms. If the wave functions have the same phase, their contributions add up, resulting in a large transmission. However, if the wave functions have opposite phases, the two cross integrals annihilate, leading to nearly zero transmission. Therefore, only the bands with positive k_n , where $k_x > K$ around the \mathbf{K} point or $k_x < -K$ around the \mathbf{K}' point, contribute to electron transmission and will be revealed in the power spectrum of \tilde{G} , while the other set of bands with negative k_n will be absent in the plot. We label the bands with numbers for energies from small to large, as shown in fig. 2(b) and fig. 3(b), where the bands with negative k_n (2, 4, and 7) are marked in red. To be specific, as the energy is increased from zero, the first band ($E/t \sim 0.1$) has $k_n > 0$ and contributes to the conductance oscillations, resulting in bright spots along

this band. When the second band emerges ($E/t \sim 0.2$), since $k_n < 0$, it has no contribution to the conductance and is “missed” by the bright spots. When the third band ($E/t \sim 0.3$) appears, it has $k_n > 0$ and the bright spots “jump” to this band and the corresponding wave vector restarts from 0 following this band, and so on. This selection can also be verified from fig. 2(a). Note that for the corresponding armchair nanoribbon, all the bands contribute to the transmission indistinguishably one mode if the energy is above their bottom level.

Another interesting feature is that, below the band dispersion curve, there is a pronounced conductance peak, as shown in fig. 2(a). This occurs only when the armchair ribbon has a band gap and is mainly resulted from the interplay of the two eigenstates spanning this region.

The numerical results and analysis presented so far are with respect to graphene quantum dots with horizontal zigzag boundaries. Essentially the same phenomena have been observed for and the same analysis applies to dots with horizontal armchair boundaries.

To conclude, we have uncovered a type of conductance oscillations in graphene quantum dots, which are caused exclusively by variation in the geometry of the device, and we have provided systematic computational results and a physical theory to demonstrate that the oscillations can be explained by the energy-band structure of the graphene ribbon associated with the underlying quantum dot. The bands on which the conductance oscillation scars are determined by the phase of the wave function for the two set of atoms, where only those with the same phase have contributions. From an applied standpoint, our finding has direct implications to devices where the device is large and the leads are relatively small thus an accurate alignment of the lead to the device is highly nontrivial. The conductance of the device can depend sensitively on the location of the leads and the Fermi energy. Such a sensitive dependence can be employed for a control scheme [17] for manipulation of electron beam propagation [18] as one can apply small perturbations, *e.g.*, the lead position or the Fermi energy, to generate a desired conductance change.

This work was supported by AFOSR under Grant No. FA9550-09-1-0260 and by ONR under Grant No. N00014-08-1-0627. LH was also supported by NSFC under Grant No. 11005053. We thank Drs D. K. FERRY, S. M. GOODNICK and R. AKIS for helpful discussions.

REFERENCES

- [1] BEENAKKER C. W. J., *Rev. Mod. Phys.*, **80** (2008) 1337; CASTRO NETO A. H., GUINEA F., PERES N. M. R., NOVOSELOV K. S. and GEIM A. K., *Rev. Mod. Phys.*, **81** (2009) 109.
- [2] YAZYEV O. V. and KATSNELSON M. I., *Phys. Rev. Lett.*, **100** (2008) 047209; XIA F., MUELLER T., LIN Y.-M., VALDES-GARCIA A. and AVOURIS P., *Nat. Nanotechnol.*, **4** (2009) 839; ZHU J., JHAVERI R. and WOO J. C. S., *Appl. Phys. Lett.*, **96** (2010) 193503; YU D. and DAI L., *Appl. Phys. Lett.*, **96** (2010) 143107.
- [3] DAN Y., LU Y., KYBERT N. J., LUO Z. and JOHNSON A. T. C., *Nano Lett.*, **9** (2009) 1472; POSTMA H. W. CH., *Nano Lett.*, **10** (2010) 420; MOHANTY N. and BERRY V., *Nano Lett.*, **8** (2008) 4469; COHEN-KARNI T., QING Q., LI Q., FANG Y. and LIEBER C. M., *Nano Lett.*, **10** (2010) 1098.
- [4] BOLOTIN K. I., SIKES K. J., JIANG Z., KLIMA M., FUDENBERG G., HONE J., KIM P. and STORMER H. L., *Solid State Commun.*, **146** (2008) 351.
- [5] ZHANG L. M. and FOGLER M. M., *Phys. Rev. Lett.*, **100** (2008) 116804; WILLIAMS J. R., DICARLO L. and MARCUS C. M., *Science*, **317** (2007) 638; LEMME M. C., ECHTERMAYER T. J., BAUS M. and KURZ H., *IEEE Electron Device Lett.*, **28** (2007) 282.
- [6] BUNCH J. S., YAISH Y., BRINK M., BOLOTIN K. and MCEUEN P. L., *Nano Lett.*, **5** (2005) 287; UJIE Y., MOTOOKA S., MORIMOTO T., AOKI N., FERRY D. K., BIRD J. P. and OCHIAI Y., *J. Phys.: Condens. Matter*, **21** (2009) 382202; VENUGOPAL A., COLOMBO L. and VOGEL E. M., *Appl. Phys. Lett.*, **96** (2010) 013512.
- [7] KRSTI V., OBERGFELL D., HANSEL S., RIKKEN G. L. J. A., BLOKLAND J. H., FERREIRA M. S. and ROTH S., *Nano Lett.*, **8** (2008) 1700; YU Y.-J., ZHAO Y., RYU S., BRUS L. E., KIM K. S. and KIM P., *Nano Lett.*, **9** (2009) 3430; LEE E. J. H., BALASUBRAMANIAN K., WEITZ R. T., BURGHARD M. and KERN K., *Nat. Nanotechnol.*, **3** (2008) 486.
- [8] LIANG G., NEOPHYTOU N., LUNDSTROM M. S. and NIKONOV D. E., *Nano Lett.*, **8** (2008) 1819; WANG Q. J. and CHE J. G., *Phys. Rev. Lett.*, **103** (2009) 066802; BARRAZA-LOPEZ S., VANEVIĆ M., KINDERMANN M. and CHOU M. Y., *Phys. Rev. Lett.*, **104** (2010) 076807.
- [9] TAKAGAKI Y. and PLOOG K. H., *Phys. Rev. B*, **57** (1998) 12689(R).
- [10] KATSNELSON M. I. and GUINEA F., *Phys. Rev. B*, **78** (2008) 075417.
- [11] BIRD J. P., AKIS R., FERRY D. K., VASILESKA D., COOPER J., AOYAGI Y. and SUGANO T., *Phys. Rev. Lett.*, **82** (1999) 4691.
- [12] See, for example, IMRY Y., *Europhys. Lett.*, **1** (1986) 249; LEE P. A., STONE A. D. and FUKUYAMA H., *Phys. Rev. B*, **35** (1987) 1039; KETZMERICK R., *Phys. Rev. B*, **54** (1996) 10841; JALABERT R. A., BARANGER H. U. and STONE A. D., *Phys. Rev. Lett.*, **65** (1990) 2442; PRIGODIN V. N., EFETOV K. B. and IIDA S., *Phys. Rev. Lett.*, **71** (1993) 1230; SACHRAJDA A. S., KETZMERICK R., GOULD C., FENG Y., KELLY P. J., DELAGE A. and WASILEWSKI Z., *Phys. Rev. Lett.*, **80** (1998) 1948.
- [13] DATTA S., *Electronic Transport in Mesoscopic Systems* (Cambridge University Press, Cambridge, UK) 1995.
- [14] BREY L. and FERTIG H. A., *Phys. Rev. B*, **73** (2006) 235411.
- [15] WAKABAYASHI K., FUJITA M., AJIKI H. and SIGRIST M., *Phys. Rev. B*, **59** (1999) 8271.
- [16] FERRY D. K., GOODNICK S. M. and BIRD J., *Transport in Nanostructures* (Cambridge University Press, New York) 1997.
- [17] OTT E., GREBOGI C. and YORKE J. A., *Phys. Rev. Lett.*, **64** (1990) 1196.
- [18] WANG Z. and LIU F., *ACS Nano*, **4** (2010) 2459.